Photonic Sensors (2013) Vol. 3, No. 1: 52–56

DOI: 10.1007/s13320-012-0082-3 **Photonic Sensors**

Regular

Temperature-Independent Torsion Sensor Based on "Figure-of-Eight" Fiber Loop Mirror

Ricardo M. SILVA[1], António B. Lobo RIBEIRO[2], and Orlando FRAZÃO[1*]

[1]*INESC Porto, Rua do Campo Alegre 687, 4169-007 Porto, Portugal, Departamento de Física da Faculdade de Ciências da Universidade do Porto, Rua do Campo Alegre 687, 4169-007 Porto, Portugal*

[2]*Faculty of Health Sciences, University Fernando Pessoa, R. Carlos da Maia 296, 4200-150 Porto, Portugal*

[*]Corresponding author: Orlando FRAZÃO E-mail: ofrazao@inescporto.pt

Abstract: An interrogation sensor system combining the "figure-of-eight" fiber loop mirror using a single directional 3×3 fiber optic coupler was proposed. One fiber loop mirror was formed by inserting a length of high birefringent optical fiber at the input ports of the 3×3 coupler. Splicing the output ports of the 3×3 coupler between them created the other fiber loop mirror. The introduction of this second loop gave rise to two polarization states of light with the same frequency but different optical phase. The mechanical torsion sensing head was located at the second loop and was exhibited an average modulus torsion sensitivity of 7.9×10^{-4} degree/dB. The performance of the sensor was not affected by environmental temperature variations.

Keywords: Torsion sensor, fiber loop mirror, interferometer

Citation: Ricardo M. SILVA, António B. Lobo RIBEIRO, and Orlando FRAZÃO, "Temperature-Independent Torsion Sensor Based on 'Figure-of-Eight' Fiber Loop Mirror," *Photonic Sensors*, vol. 3, no. 1, pp. 52–56, 2013.

1. Introduction

Nanostrain measurements can be useful in specific applications such as geophysics engineering.

Since the end of the 1980s, the fiber loop mirror (FLM) has been demonstrated as an attractive device for optical fiber sensing [1]. Traditionally, the FLM was made up of a splice between the output ports of a 2×2, 3-dB directional fiber optic coupler. In this case, the two waves traveled within identical optical path lengths in opposite directions, and a constructive interference was assured when the waves recombined at the coupling region. Then, all light was reflected back into the input port, while none was transmitted to the output port. When a section of the highly birefringent (HiBi) optical fiber was spliced inside the FLM, a path imbalance was introduced between the light that propagated along different polarization eigenaxes, and an interferometric channeled spectrum was observed at the output.

In 1997 [2], the first high birefringent fiber loop mirror (HiBi FLM) for temperature measurement was reported. The configuration consisted of a 2×2, 3-dB polarization maintaining fiber coupler, fabricated with a bow-tie fiber. By cross splicing the output ports at an angle, it was guaranteed that both port lengths were different, forming an unbalanced Sagnac loop interferometer. This temperature sensor could operate both in transmission and reflection, and its operation did not depend on the light

Received: 17 July 2012 / Revised version: 28 July 2012

polarization at the input port [2, 3].

Recently, two new configurations of HiBi FLMs with an output port probe were proposed [4]. Both configurations using two 2×2, 3-dB couplers were spliced in between, with unbalanced arms, and one output port was used as the probe sensor. The difference between them was the location of the HiBi fiber section length. The sensing probe was characterized when subject to strain and also as an optical refractometer. A fiber optic gyroscope using a directional 3×3 fiber coupler was proposed and experimentally demonstrated by S. K. Sheem in 1980 [5]. One year later, the same author analyzed interferometric configurations utilizing 3×3 directional couplers [6]. The optical characteristics of such interferometers were compared with conventional ones using 2×2, 3-dB optical couplers.

In 1982, R. G. Priest made an analysis of the properties of the 3×3 fiber coupler reveling that four parameters were required to characterize the power transfer properties of this type of fiber coupler [7].

Johnson *et al*. [8] reported a new technique to interrogate and multiplex the fiber Bragg grating (FBG), in 2000. This technique combined a scanning band pass filter used to multiplex by wavelength various gratings in a single fiber and an unbalanced Mach-Zehnder fiber interferometer made by a 3×3 coupler to strain induced wavelength shifts.

In 2005, for the space interferometry application, a breadboard demonstrator of the fringe sensor based on a directional 3×3 optical coupler was built and tested [9]. A different technique was proposed to demodulate output signals of a directional 3×3 fiber optic coupler eliminating the dependence on the idealization of these couplers, providing enhanced tolerance to the variance of photoelectric converters [10]. A torsion sensor demodulated by the HiBi FBG was studied [11]. The intensity ratio from two reflected Bragg wavelengths was associated with the twist angle of the measured HiBi fiber. Jiang [12] in 2007, demonstrated a four element hydrophone array system using an FBG laser system. The demodulation technique for the array combined a 3×3 coupler based interferometer and three wavelength division multiplexers (WDM), believing in a new approach to use a WDM and a unique arithmetic method.

In 2008, a Sagnac interferometer with a section of a polarization maintaining side-hole fiber for multiparameter measurement was reported [13]. The sensor was experimentally demonstrated to be sensitive to torsion, temperature, and longitudinal strain, simultaneously. Theoretical and experimental results for a 3×3 Mach-Zehnder interferometer using a new unbalance differential optical detection method for the optical coherence tomography application were reported by Mao *et al*. [14].

In this paper, a new interrogation system, "figure-of-eight" fiber loop mirror, based on a single directional 3×3 fiber optic coupler is investigated. Due to the characteristics of this configuration, with two opposite loops, it is possible to perform torsion measurements independently of temperature variations of the sensor head.

2. Experimental results

Figure 1 presents the experimental setup. To illuminate the configuration, an optical broadband source with a spectral bandwidth (FWHM) of 100 nm centered at 1550 nm was placed at one of the input fiber ports of the 3×3 fiber optic coupler. With the remaining input ports, a HiBi FLM was formed [loop (1) in Fig. 1] using an elliptical core fiber (e-core, ref: 48280 1550S 5) spliced between the two ports. The HiBi fiber inserted had a physical length of 1 m, and its cross section [15] is shown in Fig. 1. The typical parameters of the e-core fiber were the group birefringence of 3.85×10^{-4} and the beat length of 4.0 mm. The polarization controller (PC) was located in the HiBi FLM region, acting as a polarization state rotator for both clockwise and

counterclockwise propagating beams.

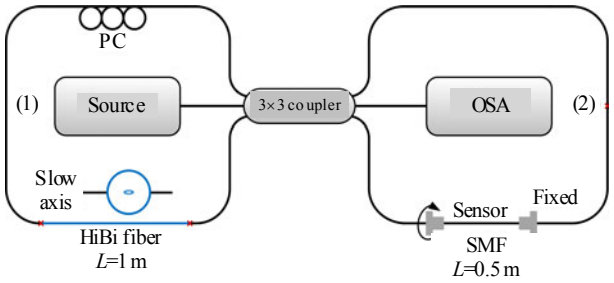

Fig. 1 Schematic of the experimental setup, exhibiting the cross-section of the HiBi fiber on the FLM(1).

At one of the output ports of the 3×3 fiber optic coupler, there was an optical spectrum analyzer (OSA) utilized to measure the transmission spectra with a maximum spectral resolution of 0.5 nm. A splice was made between the two other ports, creating the second FLM (2). With the insertion of this FLM, two polarization states of light were generated. The sensing head was located in the FLM region. The function of the HiBi FLM (1) was to optically interrogate the sensor. From Fig. 2, several spectral responses could be distinguished, which resulted from changing one paddle on the PC device. The two polarization states mentioned before are represented by the more intense (dash line) and the less intense (dot line) in the figure. It can be observed that the frequency is the same for both, but a phase difference of $\pi/2$ is noticed. When the two polarization states interfered, due to the frequency and phase difference, they gave rise to the remaining spectral responses observed in Fig. 2. While the paddle of the PC device was moved, the interference varied according to the arrow indicated in Fig. 2. The spectral response where the interference between the two polarization states was visible (dash-dot line of Fig. 2) was used to perform torsion measurements. These were done by placing the sensing head between two twist stages in the region of the FLM (2) with a length separation of 0.5 m. The torsion was only performed in one of the twist stages, while the other was kept fixed, as illustrated in Fig. 1. All measurements were performed at room temperature (~25 ℃). As the torsion was applied, an amplitude variation of the spectrum was verified, which induced a change on the amplitude of the fringes. In Fig. 3(a), the variation in the amplitude for two different angles is exhibited. For instance, it is observable that the fringe at 1548 nm (smaller rectangle) has a lower variation in the amplitude than the one placed at 1551 nm (larger rectangle). Figure 3(b) presents the fast Fourier transform (FFT), where two different frequencies can be identified. The two distinct beat frequencies were analyzed at 0.15 #/nm and 0.30 #/nm, where #/nm is the number of fringes per nanometer. Even though the frequencies were relatively close to each other, their behaviors in respect to torsion were very different. When the torsion was applied, the polarization of light was altered having transfer of light from one polarization to another. Figure 4(a) shows the amplitude behavior, determined through the FFTs, towards the torsion angles. For the torsion range of [–210º, +210º], the two frequencies had a similar response but quite different behaviors in the amplitude variation. Figure 4(b) presents the difference between the two torsion responses observed in Fig. 4(a). In this figure, four linear regions associated with different ranges of torsion angles are obtained, and their sensitivities are presented in Table 1. Twisting either to the left or to the right, for the same torsion range, similar sensitivities were obtained. Thus, with this setup, it was not possible to distinguish the direction of the applied torsion. Nevertheless, the average modulus of torsion sensitivity was 7.9×10^{-4} degree/dB. The difference between the frequencies provided elimination of the power fluctuations. This characteristic allows obtaining a torsion sensor immune to power fluctuations that can happen in the optical source. To test the temperature insensitivity of the torsion sensor, the system was placed into a tubular oven, which permitted the temperature to be set with an error smaller than 0.1 ℃. Figure 5 shows the sensing head response to temperature with a sensitivity of 4.1×10^{-6} ℃/dB, which for a variation of 30 ℃ caused an equivalent spectral change when

torsion angle varied 0.2º. Figure 5 (inset plot) shows the spectral response when the sensing head was subjected to temperatures of +25.2 ℃ and +54.4 ℃. From these results, it could be noticed that the fringe amplitude presents very low dependence on the temperature. This behavior was similar to the one reported in the literature [16]. The lack of temperature sensitivity is an important feature for the application of this configuration as a torsion sensor.

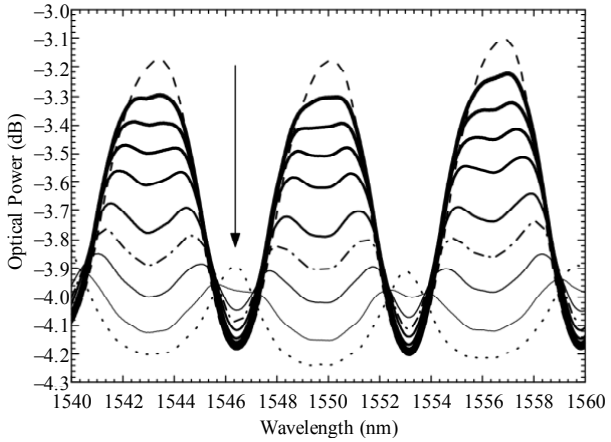

Fig. 2 Channeled spectrum of the sensing configuration when one paddle of the polarization controller was moved.

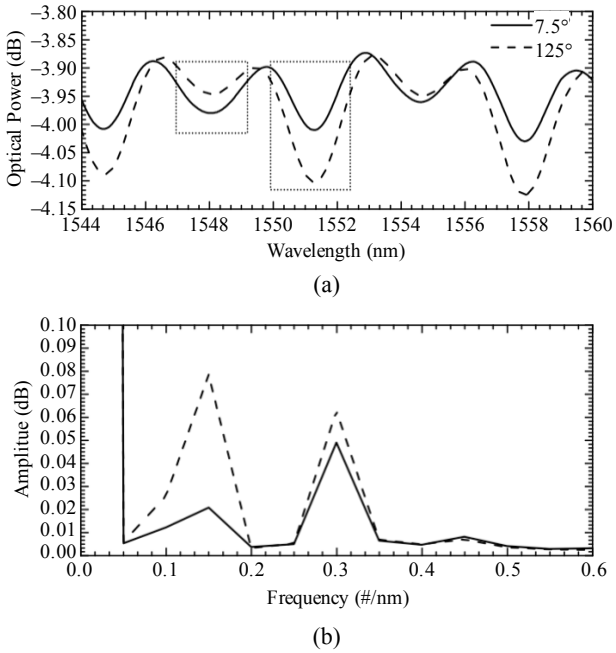

Fig. 3 FFT of the sensing head: (a) channeled spectrum for torsion angles of 7.5º and 125º, applied to the sensor head and (b) FFT analysis for the referred angles.

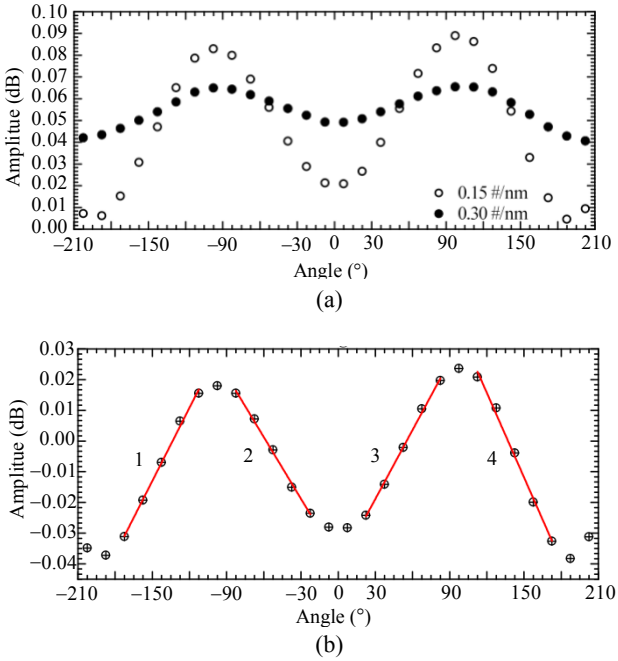

Fig. 4 Difference of the two signal frequencies: (a) sensor head response when torsion was applied and (b) the difference between the two frequencies.

Table 1 Torsion sensitivities obtained from the four slopes of Fig. 4(b).

N	Torsion range	Sensitivities °/dB
1	[−180°, −105°]	8.0×10^{-4}
2	[−85°, −20°]	-6.7×10^{-4}
3	[20°, 85°]	7.5×10^{-4}
4	[105°, 180°]	-9.2×10^{-4}

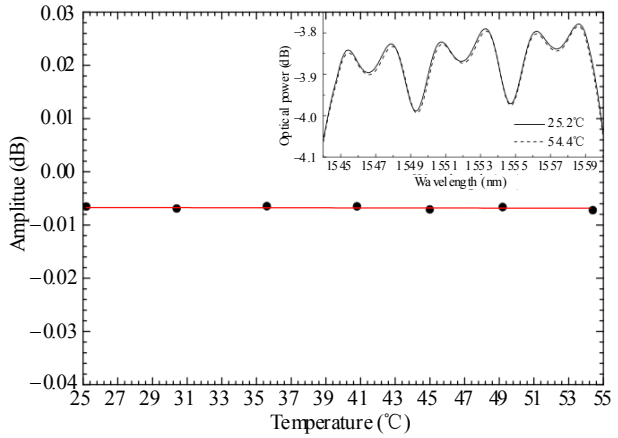

Fig. 5 Response of the sensor head to temperature (inset plot: channeled spectrum for the temperatures of +25.2 ℃ and +54.4 ℃).

3. Conclusions

To summarize, a sensing configuration based on

the "figure-of-eight" fiber loop mirror, one made by the HiBi fiber and the other by the standard single mode fiber, was demonstrated. Due to the setup configuration, two different states of polarization were observed. With the adjustment of the channeled spectrum using a PC device, these polarizations tended to interfere with each other, given the same frequency but with a phase difference of $\pi/2$. Torsion and temperature measurements were done by analysis of the FFT amplitude for two different frequencies. It was observed that the amplitude of the fringes in the channeled spectra was very sensitive to torsion. According to the FFT analysis, the lower frequency proved to be the most sensitive, and the same behavior was observed for the other frequency. Concerning to the temperature measurements, the sensing head presented very low sensitivity to these variations. This sensing configuration provided not only the elimination of the optical power fluctuations that could occur, but also temperature independence.

References

[1] D. B. Mortimore, "Fiber loop reflectors," *Journal Lightwave Technology*, vol. 6, no. 7, pp. 1217–1224, 1988.

[2] E. DelaRosa, L. A. Zenteno, A. N. Starodumov, and D. Monzon, "All-fiber absolute temperature sensor using an unbalanced high-birefringence Sagnac loop," *Optics Letters*, vol. 22, no. 7, pp. 481–483, 1997.

[3] A. N. Starodumov, L. A. Zenteno, D. Monzon, and E. DeLaRosa, "Fiber Sagnac interferometer temperature sensor," *Applied Physics Letters*, vol. 70, no. 1, pp. 19–21, 1997.

[4] O. Frazao, R. M. Silva, and J. L. Santos, "High-birefringent fiber loop mirror sensors with an output port probe," *IEEE Photonic Technology Letters*, vol. 23, no. 2, pp. 103–105, 2011.

[5] S. K. Sheem, "Fiber-optic gyroscope with [3×3] directional coupler," *Applied Physics Letters*, vol. 37, no. 10, pp. 869–871, 1980.

[6] S. K. Sheem, "Optical fiber interferometers with [3×3] directional-couplers-analysis," *Journal of Applied Physics*, vol. 52, no. 6, pp. 3865–3872, 1981.

[7] R. G. Priest, "Analysis of fiber interferometer utilizing 3×3 fiber coupler," *IEEE Journal of Quantum Electronics*, *v*ol. 18, no. 10, pp. 1601–1603, 1982.

[8] G. A. Johnson, M. D. Todd, B. L. Althouse, and C. C. Chang, "Fiber Bragg grating interrogation and multiplexing with a 3×3 coupler and a scanning filter," *Journal Lightwave Technology*, vol. 18, no. 8, pp. 1101–1105, 2000.

[9] L. K. Cheng, R. Koops, A. Wielders, and W. Ubachs, "Development of a fringe sensor based on 3×3 fiber optic coupler for space interferometry," in *Proc. SPIE*, vol. 5855, pp. 1004–1007, 2005.

[10] T. T. Liu, J. Cui, D. S. Chen, L. Xiao, and D. X. Sun, "A new demodulation technique for optical fiber interferometric sensors with [3×3] directional couplers," *Chinese Optics Letters*, vol. 6, no. 1, pp. 12–15, 2008.

[11] Y. L. Lo, B. R. Chue, and S. H. Xu, "Fiber torsion sensor demodulated by a high-birefringence fiber Bragg grating," *Optics Communication*, vol. 230, no. 4–6, pp. 287–295, 2004.

[12] Y. Jiang, "Wavelength division multiplexing addressed four-element fiber optical laser hydrophone array," *Applied Optics*, vol. 46, no. 15, pp. 2939–2948, 2007.

[13] O. Frazao, S. O. Silva, J. M. Baptista, J. L. Santos, G. Statkiewicz-Barabach, W. Urbanczyk, *et al*., "Simultaneous measurement of multiparameters using a Sagnac interferometer with polarization maintaining side-hole fiber," *Applied Optics*, vol. 47, no. 27, pp. 4841–4848, 2008.

[14] Y. Mao, S. Sherif, C. Flueraru, and S. Chang, "3×3 Mach-Zehnder interferometer with unbalanced differential detection for full-range swept-source optical coherence tomography," *Applied Optics*, vol. 47, no. 12, pp. 2004–2010, 2008.

[15] O. Frazao, J. M. Baptista, and J. L. Santos, "Recent advances in high-birefringence fiber loop mirror sensors," *Sensors*, vol. 7, no. 11, pp. 2970–2983, 2007.

[16] O. Frazao, R. M. Silva, J. Kobelke, and K. Schuster, "Temperature- and strain-independent torsion sensor using a fiber loop mirror based on suspended twin-core fiber," *Optics Letters*, vol. 35, no. 16, pp. 2777–2779, 2010.